



Enhanced skeletal muscle regrowth and remodelling in massaged and contralateral non-massaged hindlimb

Benjamin F. Miller¹, Karyn L. Hamilton¹ , Zana R. Majeed², Sarah M. Abshire^{2,3}, Amy L. Confides^{2,3}, Amanda M. Hayek², Emily R. Hunt², Patrick Shipman⁴, Frederick F. Peelor III¹, Timothy A. Butterfield^{2,3} and Esther E. Dupont-Versteegden^{2,3} 

¹Health and Exercise Science, Colorado State University, Fort Collins, CO 80523-1582, USA

²Department of Rehabilitation Sciences, College of Health Sciences, University of Kentucky, Lexington, KY 40536-0200, USA

³Center for Muscle Biology, University of Kentucky, Lexington, KY 40536-0200, USA

⁴Department of Mathematics, Colorado State University, Fort Collins, CO 80523-1582, USA

Edited by: Kim Barrett & Ylva Hellsten

Key points

- Muscle fibre cross sectional area is enhanced with massage in the form of cyclic compressive loading during regrowth after atrophy.
- Massage enhances protein synthesis of the myofibrillar and cytosolic, but not the mitochondrial fraction, in muscle during regrowth.
- Focal adhesion kinase activation and satellite cell number are elevated in muscles undergoing massage during regrowth.
- Muscle fibre cross sectional area and protein synthesis of the myofibrillar fraction, but not DNA synthesis, are elevated in muscle of the contralateral non-massaged limb.
- Massage in the form of cyclic compressive loading is a potential anabolic intervention during muscle regrowth after atrophy.

Abstract Massage, in the form of cyclic compressive loading (CCL), is associated with multiple health benefits, but its potential anabolic effect on atrophied muscle has not been investigated. We hypothesized that the mechanical activity associated with CCL induces an anabolic effect in skeletal muscle undergoing regrowth after a period of atrophy. Fischer–Brown Norway rats at 10 months of age were hindlimb unloaded for a period of 2 weeks. The rats were then allowed reambulation with CCL applied at a 4.5 N load at 0.5 Hz frequency for 30 min every other day for four bouts during a regrowth period of 8 days. Muscle fibre cross sectional area was enhanced by 18% with massage during regrowth compared to reloading alone, and this was accompanied by elevated myofibrillar and cytosolic protein as well as DNA synthesis. Focal adhesion kinase phosphorylation indicated that CCL increased mechanical stimulation, while a higher number of Pax7⁺ cells likely explains the elevated DNA synthesis. Surprisingly, the contralateral non-massaged limb exhibited a comparable 17% higher muscle fibre size compared to reloading alone, and myofibrillar protein synthesis, but not DNA synthesis, was also elevated. We conclude that massage in the form of CCL induces an anabolic response in muscles regrowing after an atrophy-inducing event. We suggest that massage can be used as an intervention to aid in the regrowth of muscle lost during immobilization.

B. F. Miller and K. L. Hamilton are co-first authors.

T. A. Butterfield and E. E. Dupont-Versteegden are co-senior authors.

(Received 9 August 2017; accepted after revision 16 October 2017; first published online 31 October 2017)

Corresponding author E. E. Dupont-Versteegden: Department of Rehabilitation Sciences, College of Health Sciences, University of Kentucky, Lexington, KY 40536-0200, USA. Email: eedupo2@uky.edu

Introduction

Muscle mass is strongly correlated with and highly predictive of morbidity and mortality (Rantanen *et al.* 2000; Metter *et al.* 2002; Wolfe, 2006; Srikanthan & Karlamangla, 2014), and we propose that massage could serve as an intervention to enhance muscle size in individuals who are unable to perform resistance exercise. Massage is defined as a mechanical manipulation of body tissues with rhythmical pressure and stroking for the purpose of promoting health and well-being (Cafarelli & Flint, 1992); many health benefits have been attributed to this manual therapy. For example, it has been shown in animals as well as humans that inflammatory pathways are attenuated by the application of rhythmic stroking (Butterfield *et al.* 2008; Crane *et al.* 2012; Waters-Banker *et al.* 2014a,b). Further, there is evidence that massage can decrease muscle atrophy since massage of facial muscles lessens atrophy and increases the tone of masticatory muscles (Balogh, 1970), and massaged muscles in a denervated cat were heavier and stronger (Suskind *et al.* 1946).

Mechanical stimuli play a major role in the regulation of muscle mass since modifications in environmental mechanical stress cause changes in the muscle that influence protein synthesis and metabolism to reflect current loading conditions (reviewed in Tidball, 2005; Marcotte *et al.* 2015). Mechanotransduction, or the ability to translate a mechanical stimulus into intracellular biochemical events, takes place at the interface between the extracellular matrix (ECM) and the muscle membrane. Integrins are the main receptors that connect the ECM with the cytoskeleton and intracellular signalling pathways, and are part of focal adhesion complexes (FACs) located at the cell membrane of muscle fibres (Katsumi *et al.* 2004; Graham *et al.* 2015). Focal adhesion kinase (FAK) is one of the components of FACs and is thought to be one of the main molecules through which integrins convey growth signals, since engagement of integrins induces phosphorylation of FAK (Spangenburg, 2009; Tomakidi *et al.* 2014; Graham *et al.* 2015). Activation of FAK occurs through autophosphorylation of tyrosine 397 and it was shown that mechanical overload increases FAK phosphorylation (Gordon *et al.* 2001) while decreased loading inhibits FAK phosphorylation. FAK modulates mTOR activity through phosphorylation and subsequent degradation of TSC2, which is a negative inhibitor of mTOR, thereby permitting phosphorylation and activation of downstream targets of mTOR such as p70s6k and 4E-BP1 (Gan *et al.* 2006; Crossland *et al.* 2013). The end result of activation of this signalling cascade is

an increase in protein synthesis in the form of enhanced translation and potentially an increase in muscle size.

Unilateral strength training (Munn *et al.* 2004; Carroll *et al.* 2006) and inflammatory lesions (Shenker *et al.* 2003; Song *et al.* 2012) have a so-called cross-over effect where the contralateral limb responds similarly to the manipulated limb. In a previous study we reported that the immunomodulatory response to massage was load-independent in the contralateral limb while the ipsilateral side reacted depending upon applied load (Waters-Banker *et al.* 2014a). The cross-over effect of resistance training is usually much smaller than the ipsilateral effect, with studies reporting that the strength gain on the contralateral side is about 35% of that on the exercised side (Yue & Cole, 1992; Munn *et al.* 2004; Song *et al.* 2012). Currently, no studies have been performed to test the potential muscle enhancing action of massage on the contralateral side, which would have great potential clinical implications, such as enhancing muscle size in limbs that are too injured to touch or exercise.

In this study we describe the effects of massage on gastrocnemius muscles of rats that are undergoing cyclic compressive loading (CCL), a massage mimetic, during a period of recovery from atrophy. We chose a rat model because the applied loads could be standardized with the CCL device, which is much more difficult to achieve in humans; in addition, in rats it is also easier to induce muscle atrophy in a more reproducible and predictable manner. We hypothesized that massage in the form of unilateral CCL enhances the muscle regrowth response after disuse in both the limb receiving CCL and the contralateral leg. Understanding the potential benefits of CCL in the rat model could help with translation of appropriate loads and frequencies to enhance muscle regrowth in atrophied human muscles.

Methods

Ethical approval

All animal procedures were conducted in accordance with institutional guidelines for the care and use of laboratory animals and were approved by the Institutional Animal Care and Use Committee of the University of Kentucky, which operates under the guidelines of the animal welfare act and the public health service policy on the humane care and use of laboratory animals. The study was conducted in adherence to the NIH *Guide for the Care and Use of Laboratory Animals*. Rats were housed in a temperature- and humidity-controlled room and maintained on a

14:10 h light–dark cycle with food and water *ad libitum*. Animals were euthanized via a lethal dosage of sodium pentobarbital (150 mg g⁻¹) injected intraperitoneally, followed by exsanguination through cardiac puncture.

Study design and animal experimentation

Animals were randomized to the groups and personnel involved in the analysis of the data were blinded to the treatment groups. Male Brown Norway–F344 rats at 10 months of age (National Institute on Aging, Bethesda, MD, USA) were housed in regular sized cages within the animal housing facility at the University of Kentucky with access to food and water *ad libitum*. The experimental design for the study is depicted in Fig. 1. Rats were randomly assigned into four groups ($n = 8$ each group): weight bearing (WB), hindlimb suspended for 14 days (HS), hindlimb suspended for 14 days followed by reambulation for 7 days (RE), and hindlimb suspended for 14 days followed by reambulation for 7 days during which the massage mimetic cyclic compressive loading (CCL) was applied to the right gastrocnemius muscle every other day starting on day 0 (REM) for a total of four bouts.

Rats in the WB and HS groups received a bolus of deuterium oxide (D₂O) (99%) at the start of the experiment, equivalent to 5% of the body water pool, followed by drinking water enriched 8% with D₂O for the remainder of the 14 day period (Miller *et al.* 2013; Drake *et al.* 2013, 2014, 2015) (Fig. 1). Rats in the RE and REM group received the same bolus of D₂O 2 days before the start of reambulation followed by 8% D₂O enriched drinking water until euthanasia for a total of 9 days. Rats were euthanized with an overdose of sodium

pentobarbital 24 h after the last bout of CCL for the REM group or at the end of the designated period for the other groups. At termination intracardiac blood was collected, gastrocnemius muscles were harvested, weighed, and flash frozen in liquid nitrogen, and bone marrow was collected from the femur using a phosphate buffered saline (PBS) flush. For rats in WB, HS and RE groups, only the right gastrocnemius muscle was harvested while for the REM group both left (REM-L) and right muscles were collected to be able to determine effects of massage on the contralateral side to the massaged limb. For further analysis, gastrocnemius muscles were cut midbelly and the distal half was mounted for tissue sectioning in a cryostat to determine muscle fibre cross sectional area (CSA) and for (immuno)histochemical analyses of cellular content. Small slices of about 50 mg were cut from the internal proximal side for determination of protein and DNA synthesis, western blot analysis and RNA determination.

Cyclic compressive loading of gastrocnemius muscle

After hind limb suspension period rats in the REM group received CCL starting at the time of reloading and continuing every other day during reambulation for a total of four bouts. Each bout consisted of 30 min of CCL over the gastrocnemius muscle at 4.5 N load and 0.5 Hz as described previously (Waters-Banker *et al.* 2014a). For application of CCL, rats were anaesthetized using isoflurane (2% isoflurane/500 ml oxygen via a nose cone) and placed dorsal recumbent on a heated sling with one limb secured to a small platform by athletic tape encircling the talocrural joint. The gastrocnemius muscle was placed facing superiorly for the

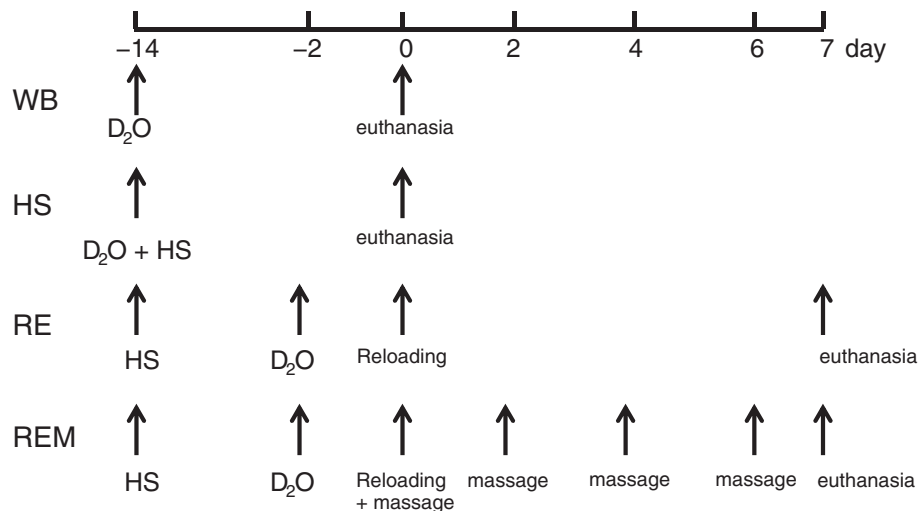


Figure 1. Experimental design for the project

HS, hindlimb suspension; RE, reambulation through reloading; REM, reambulation with massage through CCL; WB, weight bearing. D₂O indicates time points of heavy water injections. Rats received D₂O in drinking water after the injection until euthanasia.

application of CCL by a custom fabricated CCL device as described previously (Waters-Banker *et al.* 2014a). A spring loaded strut mechanism was designed to allow a cylinder to roll longitudinally over a contoured mass of tissue and displace vertically in response to the normal force exerted upwards from the tissue to the roller during an oscillating movement. A force transducer enabled continuous, real-time readings of the normal force applied to the roller. For CCL application, the roller was placed on the skin overlying the gastrocnemius muscle, immediately proximal to the lateral malleolus of the hindlimb, and cycled proximal and distal along the length of the gastrocnemius muscle at a frequency of 0.5 Hz. The contralateral left limb (REM-L) in all groups was not subjected to CCL. Rats in the RE group were anaesthetized and placed recumbent for 30 min without application of CCL (sham treatment). Upon completion of the fourth CCL session or sham treatment the rats were returned to their cages and allowed to recover for 23.5 h after which they were euthanized, using an overdose of sodium pentobarbital and exsanguination.

Determination of protein and DNA fractional synthesis rate

For analysis of protein, tissues were fractionated according to our previously published procedures (Drake *et al.* 2013, 2014, 2015). Skeletal muscle tissue was homogenized 1:10 in isolation buffer (100 mM KCl, 40 mM Tris-HCl, 10 mM Tris base, 5 mM MgCl₂, 1 mM EDTA, 1 mM ATP, pH 7.5) with phosphatase and protease inhibitors (Halt, Thermo Fisher Scientific, Waltham, MA, USA) using a bead homogenizer (Next Advance Inc., Averill Park, NY, USA). After homogenization, subcellular fractions were isolated via differential centrifugation as previously described (Drake *et al.* 2013, 2014, 2015). Once protein pellets were isolated and purified, 250 μ l 1 M NaOH was added and pellets were incubated for 15 min at 50°C while slowly mixing. For DNA analysis DNA was extracted from ~20 mg muscle or bone marrow suspension (QiAamp DNA mini kit; Qiagen, Valencia, CA, USA). Protein was hydrolysed by incubation for 24 h at 120°C in 6 M HCl. The pentafluorobenzyl-*N,N*-di(pentafluorobenzyl) derivative of alanine was analysed on an Agilent 7890A GC (Thermo Fisher Scientific) coupled to an Agilent 5975C MS (Thermo Fisher Scientific) as previously described (Drake *et al.* 2013, 2014, 2015). The newly synthesized fraction of proteins was calculated from the true precursor enrichment using plasma analysed for D₂O enrichment and adjusted using mass isotopomer distribution analysis (Busch *et al.* 2006). To determine body water enrichment, 125 μ l of plasma was placed into the inner well of an o-ring screw cap and inverted on a heating block overnight. Two microlitres of 10 M NaOH and 20 μ l of acetone were added

to all samples and to 20 μ l 0–20% D₂O standards and then capped immediately. Samples were vortexed at low speed and left at room temperature overnight. Extraction was performed by the addition of 200 μ l hexane. The organic layer was transferred through anhydrous Na₂SO₄ into GC vials and analysed via EI mode. Determination of ²H incorporation into purine deoxyribose (dR) of DNA was performed as previously described (Drake *et al.* 2013, 2014, 2015). Briefly, DNA isolated from whole tissue and bone marrow was hydrolysed overnight at 37°C with nuclease S1 and potato acid phosphatase. Hydrolysates were reacted with pentafluorobenzyl hydroxylamine and acetic acid and then acetylated with acetic anhydride and 1-methylimidazole. Dichloromethane extracts were dried, resuspended in ethyl acetate and analysed by gas chromatography–mass spectrometry as previously described (Drake *et al.* 2013, 2014, 2015). The fraction of new DNA over the labelling period was calculated using bone marrow from the same animal as the precursor enrichment since this cell type represents a fully turned-over cell population.

To account for potential non-steady state conditions, an additional calculation was made based on our recently published paper (Miller *et al.* 2015) using myofibrillar synthesis rates and tissue mass. The mass of protein at time t , $P(t)$, obeys the differential equation:

$$\frac{dP}{dt} = k_{\text{syn}} - k_{\text{deg}}P(t), \quad (1)$$

where k_{syn} is the synthesis rate, with dimensions of mass over time, and k_{deg} is the degradation constant, with dimensions of inverse time. The equilibrium mass P_{eq} is the constant solution $P(t) = P_{\text{eq}}$ to eqn (1) for which $dP/dt = 0$. That is, P_{eq} is the solution to $0 = k_{\text{syn}} - k_{\text{deg}}P_{\text{eq}}$; $P_{\text{eq}} = k_{\text{syn}}/k_{\text{deg}}$. The fractional synthesis rate (FSR) = $k_{\text{syn}}/P_{\text{eq}}$ has dimensions of inverse time, and since $P_{\text{eq}} = k_{\text{syn}}/k_{\text{deg}}$ is, in fact, equal to k_{deg} .

Writing $P(0) = P_0$, the solution of eqn (1) is:

$$P(t) = P_0 e^{-k_{\text{deg}}t} + P_{\text{eq}}(1 - e^{-k_{\text{deg}}t}). \quad (2)$$

Similarly, the mass $P^*(t)$ of enriched protein obeys the differential equation:

$$\frac{dP^*}{dt} = k_{\text{syn}} - k_{\text{deg}}P^*(t). \quad (3)$$

Using the initial condition $P^*(t) = 0$, the solution of eqn (3) is

$$P^*(t) = P_{\text{eq}}(1 - e^{-k_{\text{deg}}t}). \quad (4)$$

The mass $P(t) - P^*(t)$ of unenriched protein is given by eqn (4) subtracted from eqn (2):

$$P(t) - P^*(t) = P_0 e^{-k_{\text{deg}}t}. \quad (5)$$

In terms of the enrichment $E(t)$ at time t and the precursor enrichment E^* :

$$P^*(t) = \frac{E(t)}{E^*} P(t). \quad (6)$$

Equations (5) and (6) yield:

$$e^{-k_{\text{deg}}t} = \left(1 - \frac{E(t)}{E^*}\right) \frac{P(t)}{P_0}, \quad (7)$$

and

$$\text{FSR} = k_{\text{deg}} = -\frac{1}{t} \ln \left[\left(1 - \frac{E(t)}{E^*}\right) \frac{P(t)}{P^*} \right]. \quad (8)$$

From eqns (4), (6) and (7) we obtain:

$$P_{\text{eq}} = \frac{P^*(t)}{1 - e^{-k_{\text{deg}}t}} = \frac{\frac{E(t)}{E^*} P(t)}{1 - \left(1 - \frac{E(t)}{E^*}\right) \frac{P(t)}{P_0}}. \quad (9)$$

Finally, the (nonfractional) synthesis rate k_{syn} can be obtained from eqns (8) and (9) since

$$k_{\text{syn}} = k_{\text{deg}} P_{\text{eq}}.$$

Western analysis for determination of protein abundance

Western analysis was performed as described previously (White *et al.* 2015) and adapted as follows. A section of the gastrocnemius muscles was homogenised in radio-immunoprecipitation assay (RIPA) buffer (Boston Bioproducts, Ashland, MA, USA) with $10 \mu\text{l ml}^{-1}$ protease inhibitor cocktail (Roche, Indianapolis, IN, USA), 5 mM benzamidine, 5 mM, *N*-ethylmaleimide, 50 mM NaF, 25 mM B-glycerophosphate, 1 mM EDTA, and 1 mM phenylmethane sulfonyl fluoride added and centrifuged at 5000 *g*; for detection of Forkhead box O3a (FOXO3a), samples were sonicated before centrifugation. Protein concentration of homogenates was determined using the bicinchoninic acid protein assay (Bio-Rad, Hercules, CA, USA). For quantification of protein abundance, 30 μg total protein was loaded and separated on 4–15% acrylamide gradient gels (Bio-Rad), followed by transfer of proteins to polyvinylidene difluoride membranes with 0.22 μm pore size (Millipore, Burlington, MA, USA). Gels intended for detection of FAK and p-FAK were transferred in 10% methanol buffer to facilitate transfer of high molecular mass proteins. Membranes were incubated in Odyssey Blocking Buffer (Li-Cor, Lincoln, NE, USA) followed by incubation with the appropriate primary antibody overnight at 4°C. The following primary antibodies were used: heat shock protein (HSP) 70 (cat. no. ADI-SPA-80; 1:1000) from Enzo Life Sciences (Farmingdale, NY, USA), total extracellular signal-regulated kinase (ERK) 1/2 (cat. no. 9102; 1:1000), p-ERK1/2 (Thr202/Tyr204) (cat.

no. 9101; 1:1000), total FAK (cat. no. 3285; 1:1000), p-FAK (tyr397) (cat. no. 3283; 1:1000), total ribosomal protein S6 (rpS6) (cat. no. 2217; 1:1000), p-rpS6 (Ser235/236) (cat. no. 4856; 1:1000), total Akt (cat. no. 9271; 1:1000), p-Akt (cat. no. S473; 1:1000), total glycogen synthase kinase 3 β (GSK3 β ; cat. no. 9315; 1:1000), p-GSK3 β (cat. no. 9336; 1:1000), and p-FOXO3a (Ser253) (cat. no. 9466; 1:1000) from Cell Signaling Technology (Danvers, MA, USA), and total FOXO3a (cat. no. sc-11351; 1:500) from Santa Cruz Biotechnology (Dallas, TX, USA). After primary antibody incubation, membranes were washed and further incubated with highly cross-absorbed infrared-labelled secondary antibodies for 1 h at room temperature (goat anti-rabbit (1:15,000, Licor, Lincoln, NE, USA) or goat anti-mouse (1:15,000, Invitrogen, Omaha, NE, USA)). Membranes were scanned using an Odyssey infrared imaging system (Licor) to detect specific antibody binding and to perform quantification. Ponceau S staining of the membranes was utilized to ensure equal loading.

(Immuno)histochemistry

Dystrophin. Mean fibre CSA was determined as previously described (White *et al.* 2015). Briefly, gastrocnemius cross sections were rehydrated in PBS and incubated in dystrophin antibody (1:50, Vector Laboratories, Burlingame, CA, USA) for 1 h at room temperature and overnight at 4°C. Secondary antibody (1:200, directly conjugated Texas Red goat anti-mouse; Rockland Immunochemicals, Gilbertsville, PA, USA) was applied and sections were coverslipped. Sections were counterstained with 4',6-diamidino-2-phenylindole (DAPI, 10 nM) (Invitrogen, Carlsbad, CA, USA) for nuclear detection and mounted with Vectashield fluorescence mounting medium (Vector Laboratories). Images were captured using a Zeiss AxioImager MI upright fluorescent microscope (Zeiss, Göttingen, Germany) and analysis was performed using AxioVision software (Zeiss). CSA was determined by manually tracing the dystrophin stained sarcolemma of at least 250 fibres in four different areas of the muscle. Myonuclear number was determined by counting all DAPI positive nuclei residing within the dystrophin stain by a trained, blinded assessor, as described previously (Jackson *et al.* 2015; Gallegly *et al.* 2004).

Pax7. Air-dried frozen gastrocnemius muscle sections (7 μm) were fixed in 4% paraformaldehyde as described previously (Jackson *et al.* 2012; McCarthy *et al.* 2011; Fry *et al.* 2014). Briefly, following fixation sections underwent an epitope retrieval protocol at 92°C using sodium citrate buffer (10 mM, pH 6.5). Endogenous peroxidase activity was blocked with 3% hydrogen peroxide in PBS and to reduce staining of endogenous mouse Ig, sections were blocked with a mouse on mouse kit (Vector Laboratories). Sections were then incubated

in Pax7 primary antibody (Developmental Studies Hybridoma Study Bank, Iowa City, IA, USA) at a 1:100 dilution followed by incubation with a goat anti-mouse biotin-conjugated secondary antibody (1:1000) (Jackson ImmunoResearch Laboratories, West Grove, PA, USA) and subsequently streptavidin–horseradish peroxidase (HRP; 1:100) included as part of the Tyramide Signal Amplification (TSA) kit (Invitrogen). TSA-Alexa Fluor 594 (Invitrogen) was used to visualize antibody binding. Sections were counterstained with DAPI (10 nM) (Invitrogen) for nuclear detection and mounted with Vectashield fluorescence mounting medium (Vector Laboratories). Pax7⁺/DAPI⁺ nuclei were counted by a trained, blinded investigator, and normalized per number of muscle fibres.

CD163 (ED2). Gastrocnemius cross sections (7 μm) were fixed in ice-cold acetone and blocked in 3% H₂O₂ in PBS and horse serum, followed by incubation in primary antibody overnight at 4°C. For detection of ED2⁺ macrophages (M2) CD163 antibody was used (1:200, BioRad, Hercules, CA, USA). The TSA system (Invitrogen) was used for HRP signal amplification and detection using cyanine-3 (Cy-3) according to the manufacturer's instructions. Muscle sections were then reacted with DAPI (10 nM, Invitrogen) to identify nuclei. Cells positive for CD163 and DAPI were counted and expressed per number of muscle fibres, by a trained, blinded investigator.

Lectin. To estimate the number of endothelial cells within capillaries in the muscle, lectin was used since it stains the luminal side of endothelial cells (Robertson *et al.* 2015). Briefly, muscle sections were cut and air dried. Lectin–tetramethylrhodamine (TRITC) (Sigma-Aldrich, St Louis, MO, USA, cat. no. L4889) was applied to the section and incubated, after which DAPI was applied and sections were coverslipped. Cells positive for DAPI and lectin were counted and expressed per muscle fibre number by a trained, blinded investigator.

Tcf4. Muscle sections were immunoreacted with transcription factor 4 (Tcf4) antibody to determine the number of fibroblasts (Mathew *et al.* 2011) as described previously (Fry *et al.* 2014). Briefly, sections were fixed in 4% paraformaldehyde followed by epitope retrieval at 92°C using sodium citrate buffer (10 mM, pH 6.5). Sections were then blocked in 1% blocking reagent supplied with the TSA kit and incubated in primary Tcf4 antibody (1:100, Cell Signaling Technology) overnight. Goat anti-rabbit secondary antibody (1:1000, Jackson ImmunoResearch Laboratories) was applied followed by blocking in 3% H₂O₂ and incubation with streptavidin–HRP supplied in the TSA kit (Invitrogen). Immunoreacted cells are then visualized with the Alexa 594 fluor supplied in the TSA kit. Sections were mounted and Tcf4/DAPI positive cells

were counted and expressed per muscle fibre number by a trained, blinded investigator.

IgG. In order to estimate potential damage due to CCL or reambulation, gastrocnemius muscle sections (7 μm) were reacted for IgG infiltration into myofibers as described (Zou *et al.* 2015). Briefly, sections were fixed in ice-cold acetone for 10 min and washed in PBS. Muscles were then incubated with fluorescein isothiocyanate-conjugated mouse anti-IgG (Vector Laboratories) overnight at 4°C. Slides were washed twice in 5% bovine serum albumin in PBS and then once in PBS. Lastly muscle sections were stained with DAPI and coverslipped with Vectashield mounting medium (Vector Laboratories). Five random fields from a gastrocnemius muscle section were photographed using Zeiss Axiovision acquisition software and the densitometric mean of each fibre was determined by a trained, blinded assessor using Axiovision image analysis software and expressed as IgG density inside fibre in arbitrary units (AU).

RNA isolation and real-time RT-PCR

Total RNA was isolated using mirVana miRNA Isolation Kit (Invitrogen) according to the manufacturer's instructions. RNA integrity was determined using the Agilent Bioanalyzer (Agilent Technologies, Santa Clara, CA, USA) and RNA concentration was measured using a Nano Drop (Thermo Fisher Scientific). Quantitative real-time reverse transcription polymerase chain reaction (RT-PCR) was performed using the protocols, chemistry and the amplification and detection systems of Applied Biosystems (Thermo Fisher Scientific, Foster City, CA, USA). For each sample, cDNA was synthesized from 1 μg of total RNA using iScript Reverse Transcriptase (Bio-Rad) according to the manufacturer's instructions. cDNA samples were aliquoted and stored at –80°C. Primer sequences were selected from the accession numbers in the National Center for Biotechnology Information database using the Primer Design function of the Primer Express v1.5 software (Applied Biosystems) and were as follows: 18S (M11188) forward, TTCGGACGTCTGCCCTATCAA, reverse, ATGGTAGGCACGGCGACTA; tubulin (NM_022298) forward, GGCATGGAGGAGGGAGAGTT, reverse, CCAACCTCCTCATAATCCTTCTCTAG; β 2-microglobulin (NM_012512.2) forward CGTGCTTGCCATTCAGAAAA, reverse GAAGTTGGGCTTCCCA TTCTC; muscle atrophy F-box (MaFbx) (NM_133521) forward, GACCTGCATGTGCTCAGTGAA, reverse, GGATCTGCCGCTCTGAGAAGT; muscle RING finger protein-1 (MURF1) forward, TGCCCTGCCAGCACAAC, reverse, GGATTGGCAGCCTGGAAGAT. PCR reactions for 18S, β 2-microglobulin, tubulin, MAFbx and MuRF1 were assembled using the SYBR Green PCR Master Mix, which required only the addition of cDNA

template and primers as described previously (White *et al.* 2015). Taqman Gene Expression Assay primers (Applied Biosystems) were as follows: α 7-integrin (Itga7), Rn01529354_m1 and pre-ribosomal 45S, Rn03034784_g1. PCR reactions for Itga7 and pre-ribosomal 45S were assembled using protocols from Applied Biosystems utilizing TaqMan[®] Gene Expression Master Mix and protocol (Applied Biosystems). Data points for the standard curve were generated using fourfold serial dilutions of cDNA. The reactions were performed using the ABI Prism[™] 7700 Sequence Detection System (Applied Biosystems) and the instrument's universal cycling conditions. RNA abundance for each gene of interest is expressed as a ratio normalized to the geometric mean of β 2-microglobulin, tubulin and 18S, as described previously (White *et al.* 2015).

Statistical analyses

For the comparisons of all groups one-way analysis of variance (ANOVA) was performed using SigmaPlot statistical analysis software (Systat Software, San Jose, CA, USA). If normality was not achieved for the samples, log transformations were performed before applying one-way ANOVA. In the case of statistical significance, Tukey's *post hoc* test was applied to identify the statistical differences between the groups. Student's two-sided *t* test was applied to determine differences between the right gastrocnemius and plantaris muscle of the RE group and the left leg of the REM group. No outliers were removed from the analyses. All values reported are means \pm standard error of the mean (SEM) and statistical significance was assumed at $P < 0.05$.

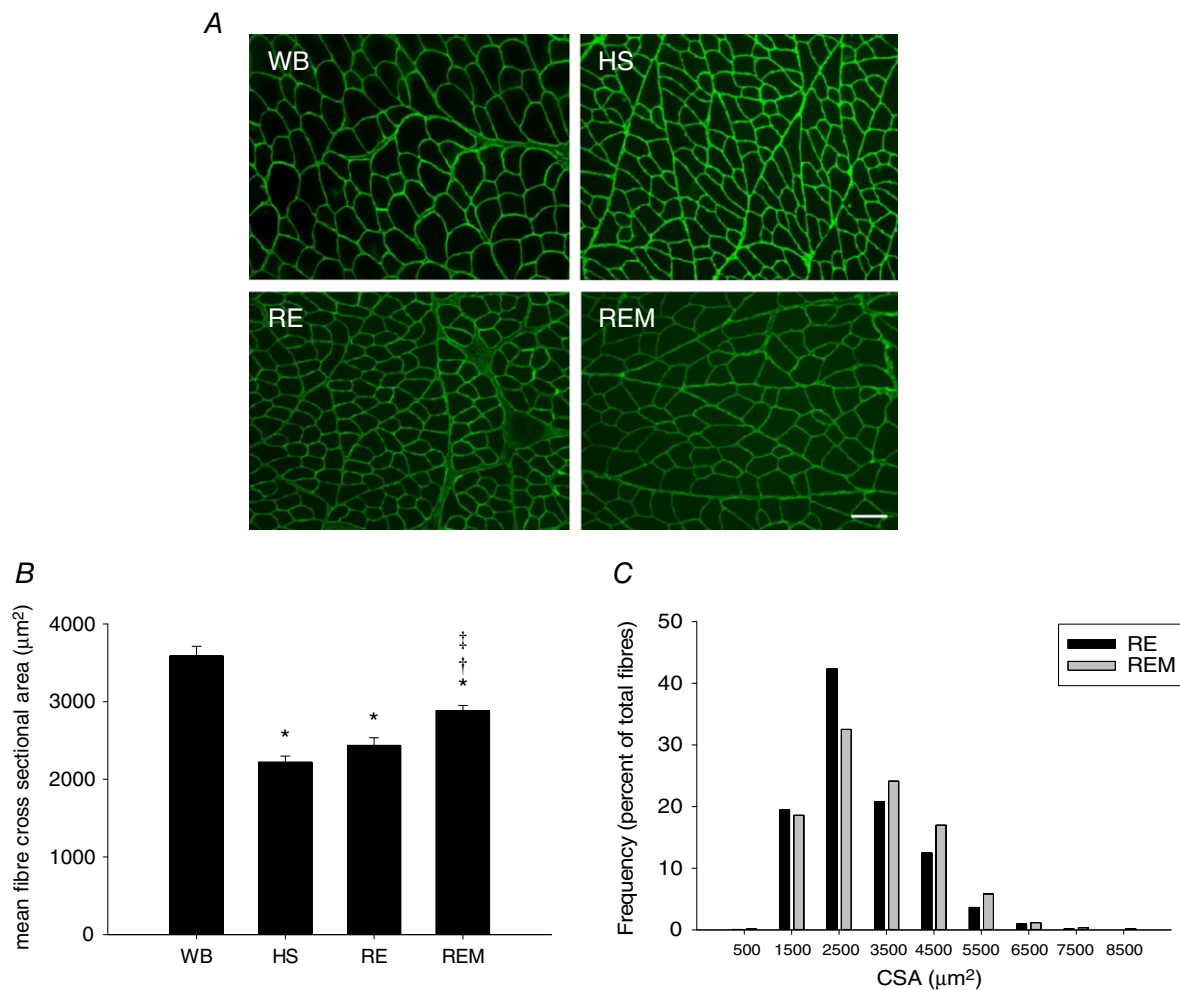


Figure 2. Massage is associated with enhanced recovery of cross sectional area (CSA) during reambulation

A, representative images of gastrocnemius muscle cross sections of WB, HS, RE and REM rats immunostained for dystrophin (green). Scale bar = 50 μ m. B and C, quantification of muscle fibre CSA of gastrocnemius from WB ($n = 8$), HS ($n = 7$), RE ($n = 8$) and REM ($n = 8$) rats (B), and frequency distribution of CSA in RE ($n = 8$) and REM ($n = 8$) rats only (C). Values are means \pm SEM. One-way ANOVA followed by Tukey's *post hoc* test was used to determine statistical significance: *different from WB, †different from HS, ‡difference from RE, $P < 0.05$.

Results

Anabolic effect of massage

Average muscle fibre CSA of gastrocnemius muscle was decreased by 38% in response to HS and 7 days of reloading did not induce a significant regrowth response (Fig. 2A and B). However, when massage in the form of CCL was applied every other day during the reloading period, muscle fibres were significantly larger compared to HS and reloading alone as evidenced from an elevated

CSA (Fig. 2B) and a shift to the right of the frequency of larger fibres in REM compared to RE (Fig. 2C). The balance between protein synthesis and breakdown of myofibrillar proteins is responsible for changes in muscle fibre size. In addition, protein synthesis and breakdown of cytosolic and mitochondrial proteins are important for the muscle to maintain efficient energy production, which makes the energetically costly process of protein synthesis and proliferation (i.e. growth) possible (Morita *et al.* 2015). Therefore, fractional synthesis rates (FSR)

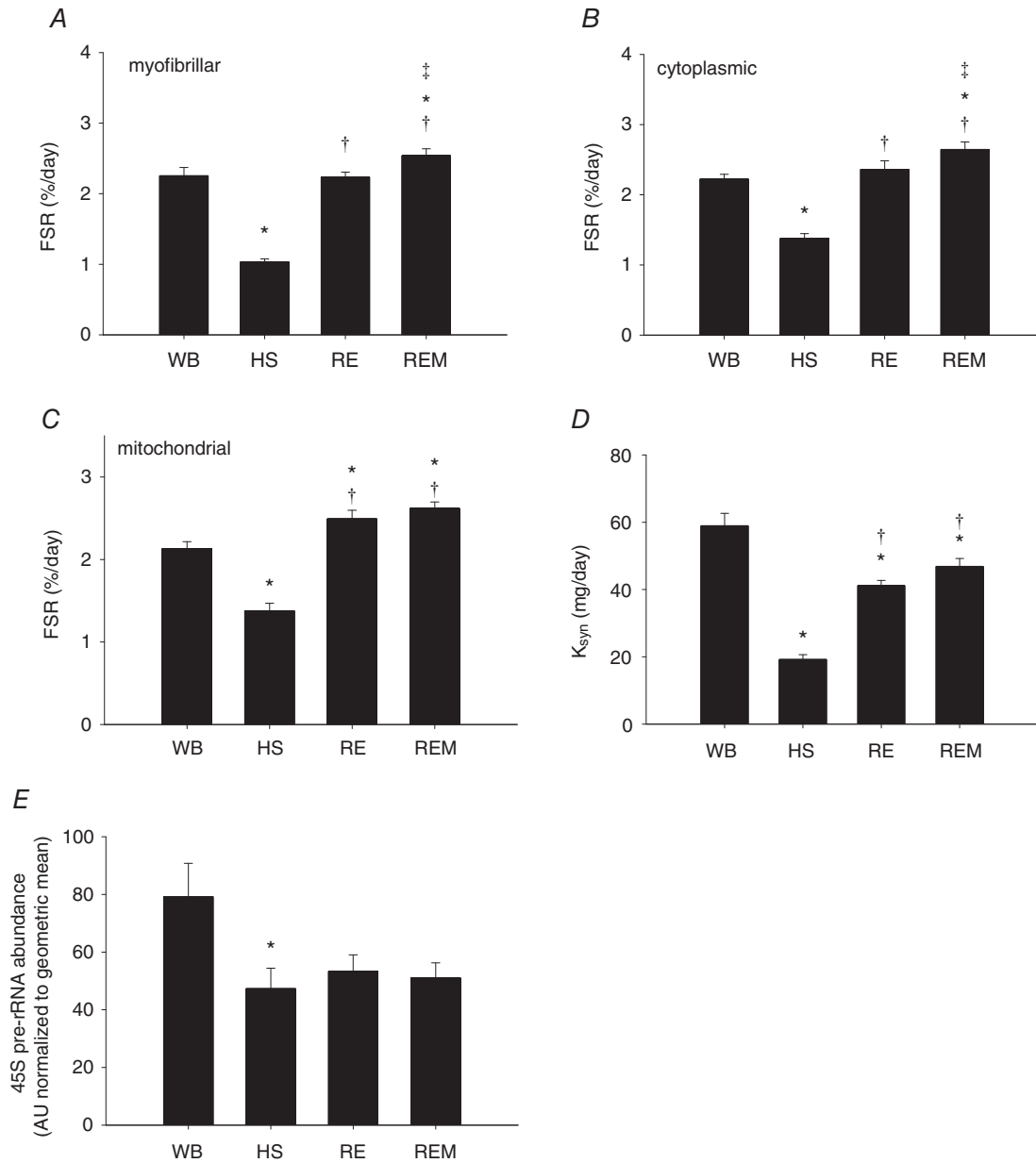


Figure 3. Protein synthesis rate is elevated by massage during reambulation

Myofibrillar (A), cytoplasmic (B), and mitochondrial (C) fractional synthesis rates (FSR), calculated protein synthesis rate, K_{syn} (D) and RNA abundance of 45S pre-rRNA (E) from gastrocnemius muscles of WB ($n = 8$), HS ($n = 7$), RE ($n = 8$) and REM ($n = 8$) rats. Values are means \pm SEM. One-way ANOVA followed by Tukey's *post hoc* test was used to determine statistical significance: *different from WB, †different from HS, ‡different from RE; $P < 0.05$.

of myofibrillar, cytosolic and mitochondrial fractions were measured directly using D₂O over the experimental period with subsequent calculation of synthesis and breakdown rates from our established model (Miller *et al.* 2015). Myofibrillar, cytosolic and mitochondrial FSR were significantly decreased by 54%, 38% and 35%, respectively, over 14 days of disuse induced by HS (Fig. 3A–C), which was likely an underestimation due to a decrease in protein pool size. Normal reambulation for 7 days restored FSR in myofibrillar and cytosolic fractions to a synthesis rate not different from control and significantly higher than HS (Fig. 3A and B); the mitochondrial fraction in RE was higher than control values (Fig. 3C). Interestingly, REM induced an enhancement of myofibrillar and cytosolic protein synthesis rates to values significantly different from reloading alone and higher than control (Fig. 3A and B), indicating that enhanced protein synthesis is most likely responsible for the increase in fibre size observed with massage during reloading.

The calculated synthesis rate (K_{syn} , mg day⁻¹) using modelling to account for non-steady state conditions and changes in protein pool size was decreased significantly by HS and reloading partially restored it, but massage did not

have an additional effect on K_{syn} (Fig. 3D). The calculation of K_{syn} demonstrated the underestimation of the decrease in protein synthesis during HS. However, the limitation of using tissue mass, rather than myofibrillar protein content, likely accounted for the subtle difference between FSR and K_{syn} for the qualitative difference of the effect of REM. 45S pre-rRNA mRNA abundance was measured as an indicator of *de novo* transcription (Cui & Tseng, 2004). Transcription was significantly decreased with HS and reloading with or without massage did not change this, indicating that the increase in FSR with massage during reloading is mostly due to an increase in translation rather than transcription.

The calculated rate parameter of protein degradation (K_{deg} , 1/*t*) showed a trend for elevation with HS, but this did not reach significance (Fig. 4A); reloading significantly decreased K_{deg} compared to WB and HS, and massage attenuated this decrease in K_{deg} , such that it was lower than HS, but not different from WB. This relative increase in K_{deg} compared to reloading is most likely due an increase in remodelling and therefore protein turnover in the massaged limb, which requires an increase in K_{deg} with a simultaneous enhancement of protein synthesis. We

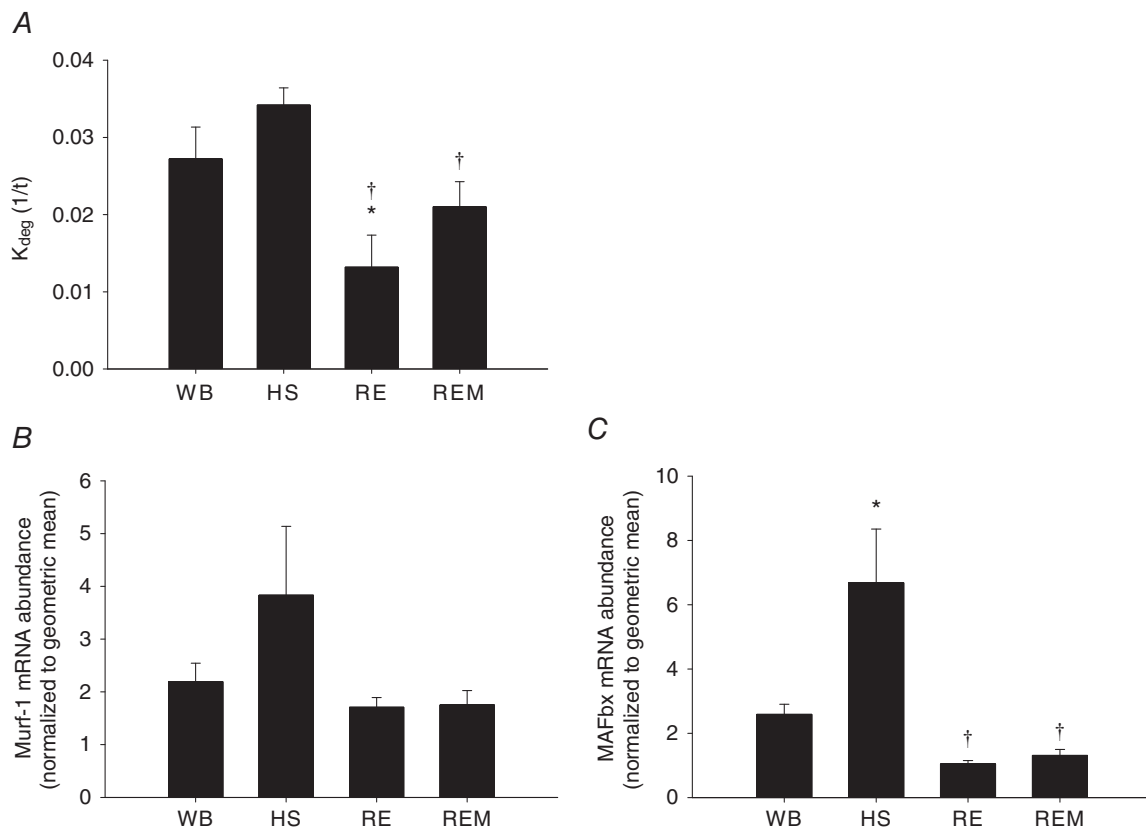


Figure 4. Effect of massage on muscle protein degradation

Calculated protein degradation rate, K_{deg} 1/*t* (A), RNA abundance of Murf-1 (B) and MAFbx (C) from gastrocnemius muscles of WB ($n = 8$), HS ($n = 7$), RE ($n = 8$) and REM ($n = 8$) rats. Values are means \pm SEM. One-way ANOVA followed by Tukey's *post hoc* test was used to determine statistical significance: *different from WB, †different from HS, $P < 0.05$.

also measured gene expression of two markers of muscle protein breakdown (Murf-1 and MAFbx, Fig. 4B and C, respectively). Both Murf-1 and MAFbx were elevated with HS, although Murf-1 failed to reach significance, and restored to control in muscles of RE rats. However, massage did not have an additional effect on MAFbx and Murf-1 levels. Taken together the protein synthesis and degradation data indicate that the regrowth promoting effect of massage is mainly due to an enhancement of myofibrillar and cytosolic protein synthesis. However, massage is also associated with an increase in K_{deg} , indicating that enhanced muscle regrowth in response to CCL also includes remodelling.

Cellular signals in response to massage

In these analyses, we do not present the ratio of phosphorylated over total protein, because this ratio is heavily influenced by changes in the abundance of total levels of the proteins, particularly by HS, which artificially inflates the ratios. Mechanical activity is sensed by the cell membrane and signalling transduction pathways induce changes in protein synthesis. Integrins play an essential role in sensing mechanical activity, because they are situated at the cell membrane connecting the intra- and extracellular space (Hynes, 2002; Katsumi *et al.* 2004). We therefore measured changes in gene expression of $\alpha 7$ -integrin (Itg7a), one of the most abundant integrins

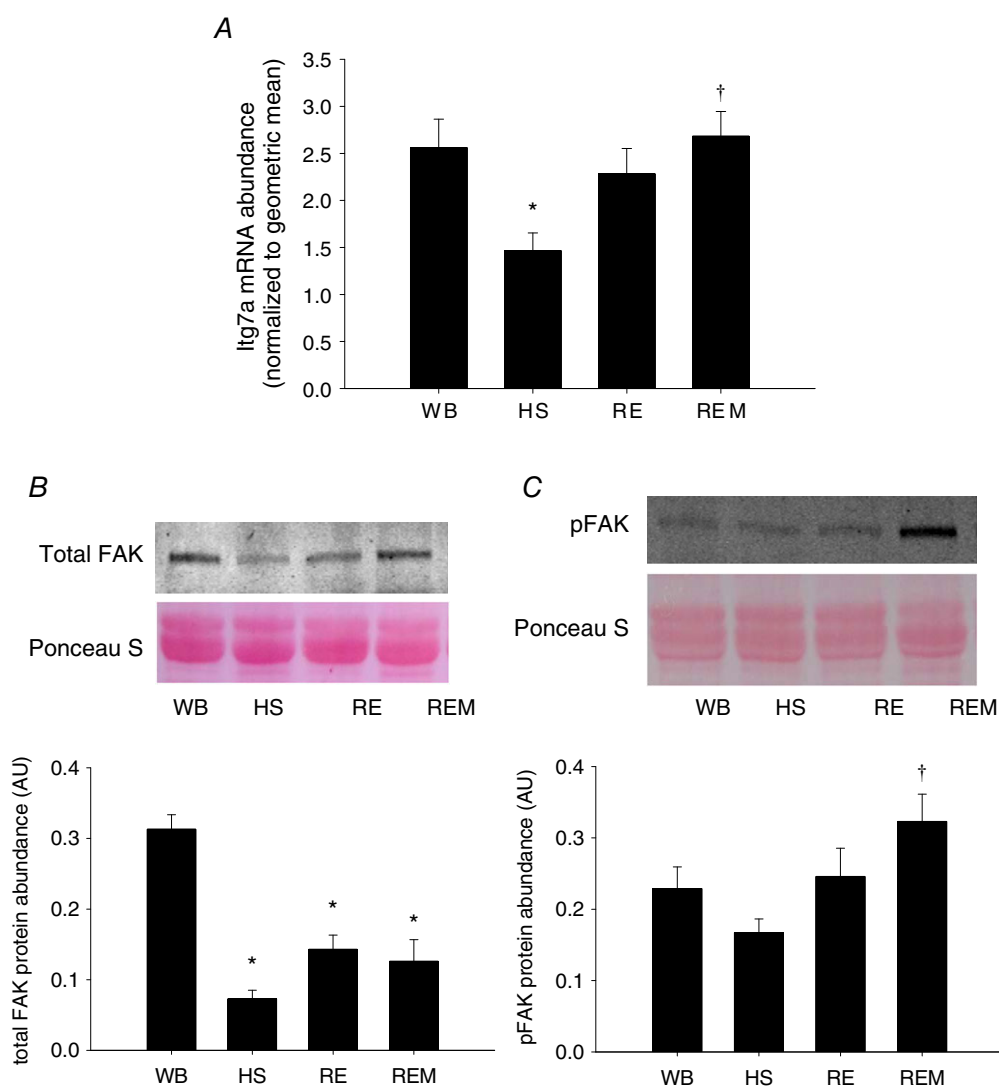


Figure 5. Mechanosensitive signalling is enhanced with massage

Gene expression of $\alpha 7$ -integrin (Itg7a) (A), representative western blot and quantification of protein abundance of FAK (B) and representative western blot and quantification of phospho-FAK (C) from gastrocnemius muscles of WB ($n = 8$), HS ($n = 7$), RE ($n = 8$) and REM ($n = 8$) rats. Values are means \pm SEM. One-way ANOVA followed by Tukey's *post hoc* test was used to determine statistical significance: *different from WB, †different from HS, $P < 0.05$.

Table 1. Western analysis of intracellular signalling pathways

	WB	HS	RE	REM
Total Akt	0.32 ± 0.04	0.14 ± 0.02*	0.23 ± 0.03	0.20 ± 0.03*
Phospho-Akt	0.52 ± 0.07	0.21 ± 0.06*	0.33 ± 0.05	0.36 ± 0.10
Total GSK3β	17.0 ± 1.6	11.2 ± 1.0	19.6 ± 2.6 [†]	22.2 ± 1.9 [†]
Phospho-GSK3β	1.8 ± 0.2	1.2 ± 0.1	2.2 ± 0.3 [†]	2.6 ± 0.2 [†]
Total ERK1/2	28.8 ± 1.7	34.1 ± 1.9	31.1 ± 2.3	38.2 ± 1.5*
Phospho-ERK1/2	1.9 ± 0.3	3.8 ± 1.1	4.0 ± 0.8	3.0 ± 0.9
Total FOXO3a	0.6 ± 0.1	0.5 ± 0.1	0.5 ± 0.1	0.6 ± 0.1
Phospho-FOXO3a	0.5 ± 0.1	0.2 ± 0.0	0.3 ± 0.1	0.4 ± 0.0
Total rps6	3259 ± 441	2882 ± 347	4047 ± 379	4774 ± 539 [†]
Phospho-rps6	970 ± 377	822 ± 308	3963 ± 677* [†]	3650 ± 854* [†]
HSP70	1.6 ± 0.3	0.7 ± 0.0	2.0 ± 0.3 [†]	2.3 ± 0.5 [†]

All values are in arbitrary density units. Values are means ± SEM. *Different from WB. [†]Different from HS.

in muscle. Itg7a was significantly decreased with HS and reloading induced an increase to levels not different from WB or HS (Fig. 5A); when massage was applied Itg7a was significantly elevated compared to HS (Fig. 5A). One of the mechanosensitive signalling pathways downstream of integrins is FAK (Graham *et al.* 2015). Total FAK was significantly decreased by HS and reloading with or without massage was not different from HS (Fig. 5B). Importantly, phosphorylated FAK, which was not changed in response to HS or RE, was significantly elevated with massage (Fig. 5C).

To investigate pathways downstream of FAK leading to the observed increase in protein synthesis, we performed western analysis for proteins involved in translation (Table 1). Total and phospho-Akt were significantly decreased with HS and recovered to a level not different from control with reloading, but massage did not enhance this response (Table 1). Similarly, total and phospho-GSK3β were elevated compared to HS with reloading without an additional effect of massage. Interestingly, abundance of total ERK1/2, which was not changed in response to HS or RE, was significantly increased with massage. However, this was not the case for phospho-ERK1/2, which did not significantly change with any of the conditions (Table 1). No change was observed under any condition in total and phospho-FOXO3a (Table 1). HSP70, which has been associated with muscle size regulation, is elevated with reloading independent of massage. Lastly, total rps6 has been suggested as an indicator of translational capacity, while phospho-rps6 is more associated with translation efficiency (Goodman *et al.* 2012). We observed no significant differences with HS, but phospho-rps6 was dramatically elevated with reloading regardless of massage, while total rps6 levels are significantly elevated compared to HS with massage, but not with reloading alone. These data suggest that massage is associated with an increase in translational capacity during reloading.

DNA synthesis and cellular identification

In addition to investigating protein synthesis we also measured DNA synthesis, which is indicative of cellular proliferation. We found that DNA synthesis was not changed with HS and RE, but in REM was significantly higher compared to WB, HS and RE (Fig. 6A). In order to identify the potential cellular basis for this elevated DNA synthesis we measured the abundance of resident macrophages (ED2⁺), endothelial cells (lectin⁺), fibroblastic cells (Tcf4⁺), and satellite cells (Pax7⁺) (Fig. 6B–E, respectively). No difference was observed in the number of ED2⁺, lectin⁺ or Tcf4⁺ cells under any of the experimental conditions (Fig. 6B–D). However, satellite cell number was significantly lower with HS and recovered with reloading to values not different from control. Moreover, the number of satellite cells was significantly elevated in REM compared to WB, HS and RE (Fig. 6E). We conclude that the elevated DNA synthesis is most likely due to a proliferation of satellite cells in the massaged gastrocnemius muscle. Interestingly, the protein to DNA synthesis ratio was decreased in the gastrocnemius muscle undergoing massage, which reached significance only for the myofibrillar fraction, indicating that remodelling in response to massage induces changes in DNA synthesis that outpace those in protein synthesis.

To investigate whether the increase in satellite cell number in the massaged limb was associated with the increase in myonuclear number and therefore fusion into the muscle fibres, we counted DAPI positive nuclei within the dystrophin labelled sarcolemma and found that there was no difference in myonuclear number between any of the groups (Fig. 7A). Since satellite cell proliferation occurs in response to muscle damage, we measured central nucleation as an indicator of regeneration in muscle and IgG infiltration as an indicator of overt damage. No changes were found in either central nuclei or IgG infiltration (Fig. 7B and C), indicating that satellite cell

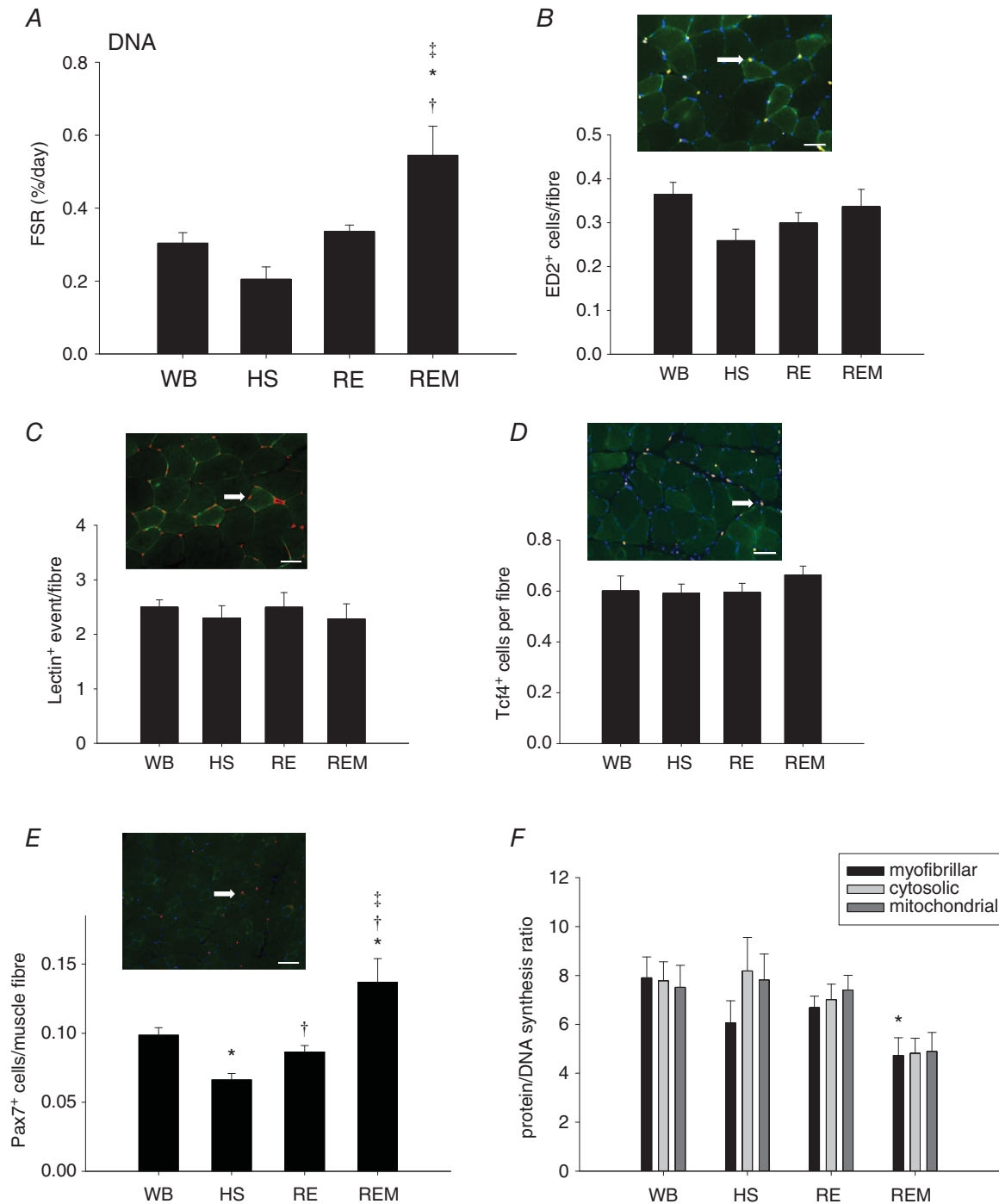


Figure 6. Increase in DNA synthesis with massage is associated with elevated number of satellite cells

Fractional DNA synthesis rate (A), representative image of ED2⁺ cells (white arrow) and number of ED2⁺ cells (B), representative image of lectin⁺ events (white arrow) and number of lectin⁺ events (C), representative image of Tcf4⁺ cells (white arrow) and number of Tcf4⁺ cells (D) and representative image of Pax7⁺ cells (white arrow) and number of Pax7⁺ cells (E) for gastrocnemius muscle of WB ($n = 8$), HS ($n = 7$), RE ($n = 8$) and REM ($n = 8$) rats. Scale bar in all images is 50 μm . Protein/DNA synthesis ratio of myofibrillar (black bar), cytosolic (light grey bar) and mitochondrial (dark grey bar) fractions from gastrocnemius muscle from WB ($n = 8$), HS ($n = 7$), RE ($n = 8$) and REM ($n = 8$) rats. Values are means \pm SEM. One-way ANOVA followed by Tukey's *post hoc* test was used to determine statistical significance: *different from WB, †different from HS, ‡different from RE, $P < 0.05$.

proliferation in this model at the applied load is not associated with overt muscle damage.

Effect of massage on contralateral and non-massaged muscles

To investigate whether massage had an effect on the contralateral non-massaged leg in the rats that received massage on the ipsilateral right gastrocnemius muscle, we investigated responses in the left leg (REM-L). Surprisingly, we found that muscle fibre cross sectional area was significantly increased in the left limb (Fig. 8A) compared to reloading alone and this was associated with a significant increase in myofibrillar, but not cytosolic or mitochondrial, protein FSR (Fig. 8B). Similar to the right leg, the increase in size and synthesis was not associated with an increase in the transcriptional marker

45S pre-rRNA (Fig. 8C), indicating that the increase in synthesis was due to an increase in translation. When accounting for changes in pool size, the calculated protein synthesis rate was not increased in the left limb compared to RE (Fig. 8D), but the calculated protein degradation was higher in the left limb (Fig. 8E), indicating that remodelling is ongoing in the non-massaged limb. Interestingly, DNA synthesis was not increased in the left gastrocnemius muscle (Fig. 8F) and neither was the number of satellite cells (Fig. 8G). Similarly, no differences were observed in any of the intracellular signalling molecules that were also measured for the right limb above (Table 2). In addition, the protein/DNA synthesis ratio for all three fractions was higher in the contralateral gastrocnemius muscle (Fig. 8H) compared to reloading alone, indicating that different mechanisms are involved in enhancing muscle fibre size in the massaged compared

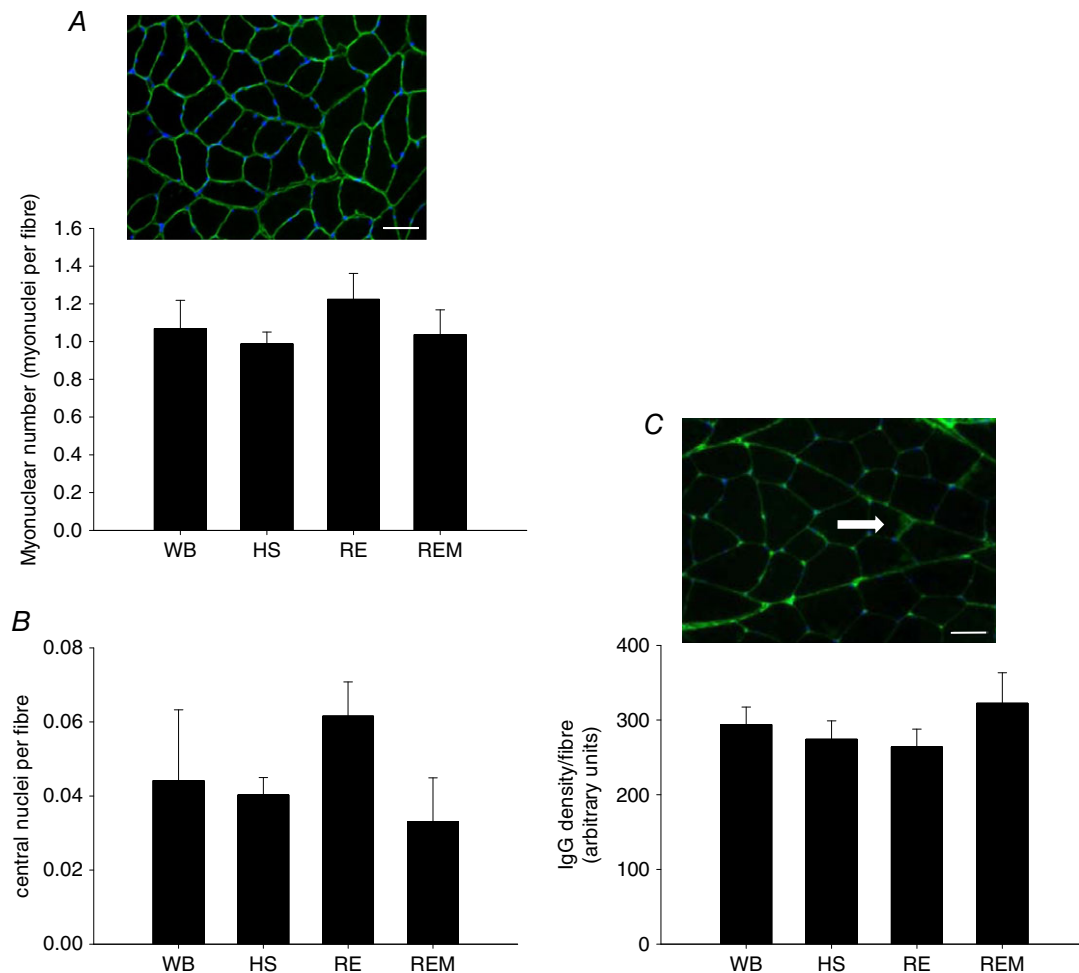


Figure 7. No increase in myonuclear number or overt damage to muscle fibres with massage

Representative image of dystrophin (green) and DAPI (blue) staining with myonuclear number (A) and central nuclei (B) quantified, and a representative image of IgG staining (green) with the white arrow pointing to intramuscular IgG, which is quantified (C) in gastrocnemius muscle of WB ($n = 8$), HS ($n = 7$), RE ($n = 8$) and REM ($n = 8$) rats. Scale bar is $50 \mu\text{m}$. Values are means \pm SEM. One-way ANOVA was used to determine statistical significance ($P < 0.05$).

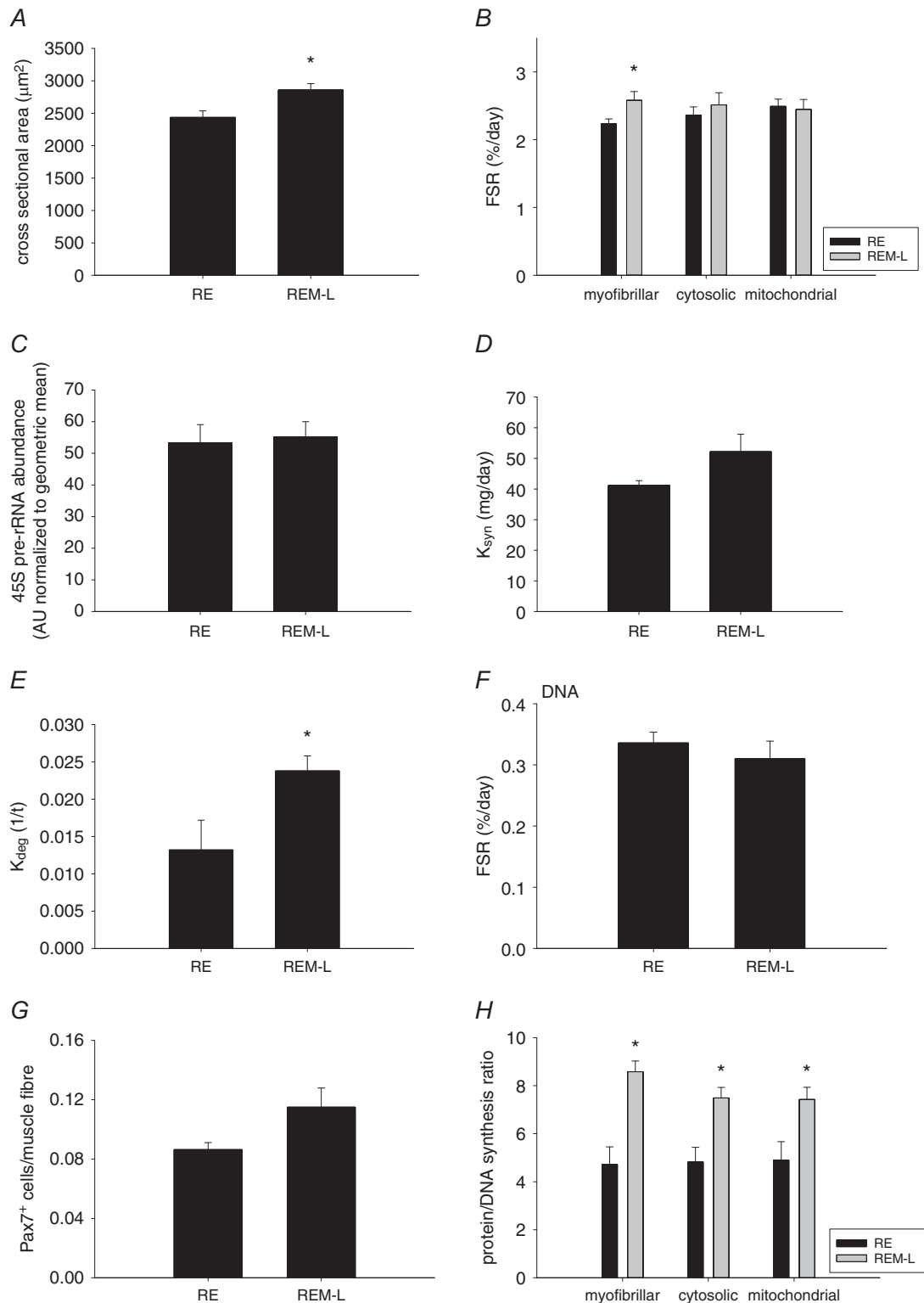


Figure 8. Massaging induces an anabolic effect in the contralateral non-massaged muscle

Mean fibre cross sectional area (A), fractional protein synthesis rate of myofibrillar, cytosolic and mitochondrial fractions (B), 45S pre-rRNA (C), calculated protein synthesis rate, K_{syn} (D), calculated protein degradation rate, K_{deg} (E), DNA synthesis rate (F), number of Pax7⁺ cells (G), and protein/DNA synthesis ratio (H) in gastrocnemius muscle from reloaded (RE, $n = 8$) rats and the contralateral left gastrocnemius from rats massaged on the right limb (REM-L, $n = 8$). Values are means \pm SEM. Two-sided t test was used to determine statistical significance: *different from RE, $P < 0.05$.

Table 2. Western analysis of intracellular signalling pathways

	RE	REM-L
Itg7a (AU normalized to geomean)	2.28 ± 0.27	2.64 ± 0.26
Murf-1 (AU normalized to geomean)	10.5 ± 0.6	9.7 ± 0.5
MAFbx (AU normalized to geomean)	0.91 ± 0.10	1.12 ± 0.13
Total FAK (AU)	0.14 ± 0.02	0.09 ± 0.02
Phospho-FAK (AU)	0.25 ± 0.04	0.29 ± 0.02
Total GSK3 β (AU)	19.6 ± 2.6	19.1 ± 1.7
Phospho-GSK3 β (AU)	2.2 ± 0.3	2.2 ± 0.2
Total ERK1/2 (AU)	31.1 ± 2.3	37.0 ± 1.9
Phospho-ERK1/2 (AU)	4.0 ± 0.8	5.6 ± 1.2
Total rps6 (AU)	4047 ± 379.3	3263 ± 515
Phospho-rps 6 (AU)	3963 ± 677	2833 ± 725
HSP70 (AU)	1.98 ± 0.33	1.48 ± 0.25

Values are means ± SEM.

to the contralateral non-massaged gastrocnemius muscle. To investigate whether a muscle that was not directly massaged would also exhibit changes on the ipsi- as well as contra-lateral side, we investigated the plantaris muscle in both limbs. In the non-massaged right plantaris muscle myofibrillar and cytoplasmic protein synthesis was elevated, but DNA synthesis was not increased (Fig. 9A–D). Interestingly, cytoplasmic and mitochondrial, as well as DNA FSR were elevated in the contralateral left limb (Fig. 9A–D), while protein/DNA synthesis ratio was not affected by massage in either limb (Fig. 9E). Similar to the results from the non-massaged contralateral gastrocnemius muscle, these data indicate that remodelling is occurring in a muscle that is not directly undergoing mechanical manipulation.

Discussion

Massage as a manual therapy to aid in the restoration of muscle size is an innovative and unique concept that carries great clinical potential, since massage can be applied in situations where exercise may not be feasible. Our novel data show that massage in the form of CCL is capable of enhancing the recovery of muscle mass after a period of disuse-induced atrophy and that this is due to increased mechanically mediated signalling, elevated protein synthesis and increased muscle remodelling. In addition, not only did the massaged limb show an anabolic response, but the contralateral, non-massaged limb was also positively affected. Although there were differences in rates of cell proliferation in the massaged *versus* contralateral non-massaged limbs, both limbs underwent significant remodelling. These findings have great potential for translation, supporting a role for massage, a simple and easy to apply intervention, for promoting enhanced muscle regrowth in clinical conditions where patients have limited mobility or unilateral pathology.

Anabolic response in massaged muscle

The enhancement of muscle cross sectional area in the massaged limb during regrowth was associated with an increase in synthesis of both the myofibrillar and cytosolic protein fractions. The increase in myofibrillar synthesis indicates that new proteins were incorporated into the sarcomeric lattice in response to massage to enhance muscle size, while the enhanced synthesis in cytosolic proteins likely is associated with changes in regulatory and signalling proteins, which are decreased during the period of disuse. The exact mechanism by which protein synthesis is enhanced is currently unknown, but our data indicate that it does not require new total transcription, since 45S rRNA was not changed with massage. However, it cannot be ruled out that specific mRNAs, which may influence the growth response, are transcriptionally regulated. The mechanotransduction signalling pathways responsible for the elevated protein synthesis with massage are not entirely clear. We collected muscle tissue and measured the involvement of some of the anabolic signalling pathways 24 h after the last bout of massage and this may have been too late to see changes in AKT or rps6 phosphorylation since most of the changes occur earlier (Baar & Esser, 1999). Also, there may have been an attenuation of the intracellular response due to repetitive bouts of massage, as occurs with resistance exercise (McGlory *et al.* 2017), such that initial elevation of levels of phosphorylation of anabolic molecules which occur after a single bout are not detected any more after multiple bouts. However, we observed elevated levels of phospho-FAK, indicating that this protein remains elevated for an extended period of time after a direct mechanical stimulus, such as massage. This is similar to the results observed in human muscle after massage in an injury model in which phospho-FAK elevation preceded changes in other pathways (Crane *et al.* 2012). The combination of elevated phospho-FAK and increased levels of integrin- α 7 mRNA indicates that

massage changed the mechanotransduction machinery in muscle, making it more responsive to mechanical signals, which translated to greater rates of protein synthesis and muscle fibre size. Of note is also that protein degradation rate was elevated in massaged muscle, as occurs with resistance exercise (McGlory *et al.* 2017), indicating that remodelling of muscle tissue occurs in response to an external mechanical stimulus. Importantly, the net effect of this remodelling was an increase in muscle fibre size.

Elevated DNA synthesis in massaged muscle

An interesting result from this study was the fact that in addition to protein synthesis, rates of DNA synthesis were also greater in muscles that were massaged during the regrowth period. We found that the most likely cell type responsible for this increase in DNA synthesis was the satellite cell, since these cells were elevated in number after massage while other cell types did not change in abundance. Satellite cells are usually activated

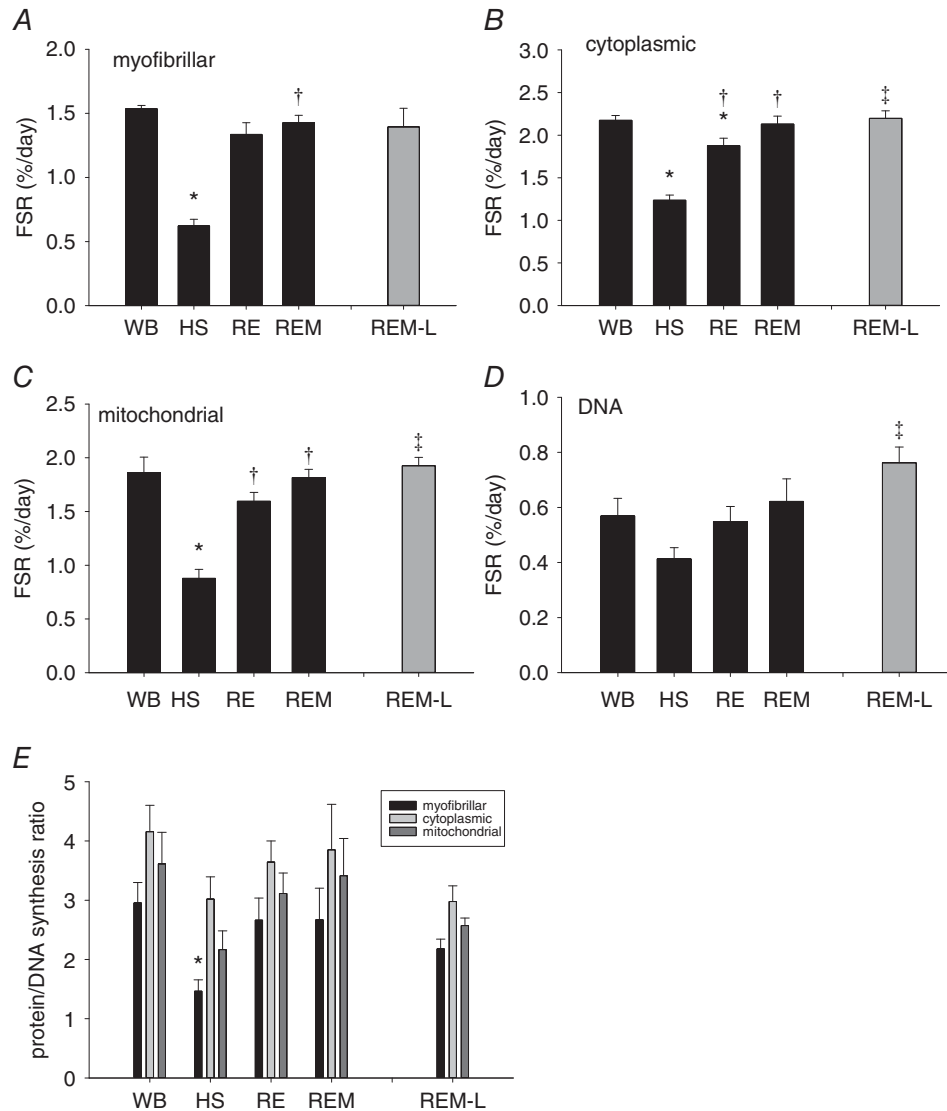


Figure 9. Changes in protein synthesis rates in response to massage in the non-massaged ipsi- and contralateral plantaris muscle

Myofibrillar (A), cytoplasmic (B), mitochondrial (C) and DNA (D) fractional protein synthesis rate in plantaris muscle of WB ($n = 8$ PS, 8 DNA), HS ($n = 9$ PS, 7 DNA), RE ($n = 8$ PS, 8 DNA), REM ($n = 8$ PS, 7 DNA) and REM-L ($n = 8$ PS, 5 DNA, grey bar) rats. Values are means \pm SEM. *Different from WB, †different from HS and ‡different from RE, $P < 0.05$. Protein/DNA synthesis ratio (E) of WB ($n = 8$), HS ($n = 7$), RE ($n = 8$), REM ($n = 7$) and REM-L ($n = 5$) rats. Values are means \pm SEM. *Different from WB. For all panels, one-way ANOVA was used to determine statistical significance between WB, HS, RE and REM and a two-sided t test was used to determine statistical significance between RE and REM-L ($P < 0.05$).

and proliferate in response to a damaging event within the muscle to repair the injured muscle fibres (Brack & Rando, 2012). However, we did not observe overt damage in response to massage, as measured by centronucleation and IgG infiltration, at the load applied in this study and as previously reported (Waters-Banker *et al.* 2014a). Therefore, we propose that satellite cells were induced to proliferate in response to the mechanical stimulus applied by the CCL. A recent paper indeed showed that higher loads during exercise were associated with an increase in myonuclear number which was attributed to activation and fusion of satellite cells (Eftestol *et al.* 2016); however, satellite cell number was not directly measured in this paper and in our study myonuclear number did not change in response to the mechanical activity indicating that satellite cell fusion likely did not occur. Many forms of hypertrophy are associated with activation and fusion of satellite cells (Westerkamp & Gordon, 2005; Ishido *et al.* 2009), but these cells are not necessary for hypertrophy (McCarthy *et al.* 2011) or regrowth (Jackson *et al.* 2012) and their requirement may depend upon the extent of hypertrophy. Regrowth after a period of atrophy has been shown to be independent of satellite cells in mice (Jackson *et al.* 2012) and therefore it was surprising that these cells increased in response to massage during regrowth in this study. The role of satellite cell proliferation in response to a mechanical stimulus such as massage without fusion to contribute to myonuclear number is therefore unclear. However, a similar phenomenon is observed during aerobic exercise in rodents as well as humans in which satellite cell number can be increased, dependent upon myosin heavy chain composition of the muscle, without a concomitant increase in myonuclear number (reviewed in Abreu *et al.* 2017) and after spinal cord injury in which activated satellite cells fail to restore myonuclear number (Dupont-Versteegden *et al.* 1999).

Massage-induced changes in contralateral muscle

Perhaps the most surprising result from this study was the observation that muscle fibre CSA and protein synthesis of the myofibrillar fraction were elevated in the non-massaged contralateral muscle compared to the gastrocnemius muscle in the reloaded rat. Cross-over effects have been observed for a number of phenomena, such as inflammatory lesions (Shenker *et al.* 2003), strength gains in response to exercise as well as electrical stimulation (Zhou, 2000; Munn *et al.* 2004; Carroll *et al.* 2006; Amiridis *et al.* 2015), regenerative and degenerative responses to muscle injury (Song *et al.* 2012), and changes in mechanomyography after exercise (McKay *et al.* 2006). In general, changes in the contralateral limb are stimulus specific, homologous and dependent upon the strength of the stimulus, and the effect on the measured outcome is almost always smaller than

on the ipsilateral side (Shenker *et al.* 2003; Munn *et al.* 2004). Even though increases in strength have been observed in contralateral muscles with unilateral exercise or electrical stimulation, changes in muscle size have not been reported. In addition, cross-over effects of massage have only been sporadically reported: we showed previously an increase in inflammatory cells in the contralateral limb (Waters-Banker *et al.* 2014a) and Jay *et al.* (2014) reported a transient decrease in muscle soreness in the contralateral muscle after massage application in humans. Mechanisms underlying this cross-over effect have not been investigated in great detail, but most studies suggest that it is neurally mediated. Recently it has been shown that sympathetic innervation is important in maintaining neuromuscular junctions and other cells in muscle (Khan *et al.* 2016) and protein synthesis can be affected by adrenergic neural pathways influencing muscle size (Navegantes *et al.* 2004). Therefore, it is possible that massage acts through the activation of the sympathetic nervous system to cause the anabolic cross-over effect and this could be achieved through direct neural mechanisms as well as endocrine-like processes. Alternatively, the cross-over effect of massage could be caused by the release of factors from muscle (myokines), such as occurs during exercise, that influence muscle (i.e. plantaris) or other organs at distant sites (Ahima & Park, 2015; Catoire & Kersten, 2015). Both possibilities require further investigation. It is clear from our study, however, that the underlying mechanism by which an increase in muscle size is obtained, is through elevated protein synthesis, even though the upstream signalling pathways leading to this anabolic response may be different between the ipsi- and contralateral side.

Protein:DNA ratio

Our labelling approach allows for simultaneous measurement of protein and DNA synthesis, and we have taken advantage of this to further explore the factors contributing to the increase in protein synthesis (Miller *et al.* 2014). When a cell proliferates there is a doubling of proteins to accommodate the daughter cell (Grebien *et al.* 2005). In whole skeletal muscle tissue, only about 40–50% of the total nuclei are myofibre nuclei, with the balance coming from cells that can be proliferative (Schmalbruch & Hellhammer, 1977; Gibson & Schultz, 1983). We use the ratio of protein:DNA synthesis to estimate how much protein synthesis is going toward proliferation rather than protein turnover in post-mitotic muscle (Miller *et al.* 2014). When this ratio increases, it is indicative of an increase in the remodelling of proteins rather than the making of new cells, whereas a decrease is indicative of an increased contribution of proliferation to the measured protein synthesis. The lower protein:DNA synthesis ratio in the myofibrillar fraction of the massaged

muscle is indicative of greater cell proliferation, which our histological analyses indicate can at least partially be accounted for by satellite cells. Therefore, there is an increase contribution of satellite cells, and potentially other proliferative cell types, that facilitate the increase in myofibrillar protein and cross sectional area. Conversely, in the contralateral limb, there was a higher protein:DNA synthesis ratio, which indicates that the increase in protein synthesis is due to remodelling of proteins in the absence of an increase in the rate of cell proliferation. These findings were supported by data from a second muscle, plantaris, in which increased protein synthesis was observed in both the massaged and non-massaged limb. Therefore, the mechanisms of muscle remodelling are not the same in the massaged *versus* non-massaged muscle, even though both show appreciable increases in protein synthesis.

Conclusion

In summary, this is the first report of massage in the form of cyclic compressive loading exerting an anabolic effect on muscles that are recovering from a period of disuse. The regrowth effect is marked both in the massaged and the contralateral limb, although the contributing mechanisms to remodelling differ in the two limbs. Since massage is a therapeutic manipulation that is generally well tolerated, the possibilities for clinical application are potentially very high in patients who are on bed rest or under non-weight-bearing orders after injury or surgery.

References

- Abreu P, Mendes SV, Ceccatto VM & Hirabara SM (2017). Satellite cell activation induced by aerobic muscle adaptation in response to endurance exercise in humans and rodents. *Life Sci* **170**, 33–40.
- Ahima RS & Park HK (2015). Connecting myokines and metabolism. *Endocrinol Metab (Seoul)* **30**, 235–245.
- Amiridis IG, Mani D, Almklass A, Matkowski B, Gould JR & Enoka RM (2015). Modulation of motor unit activity in biceps brachii by neuromuscular electrical stimulation applied to the contralateral arm. *J Appl Physiol (1985)* **118**, 1544–1552.
- Arangio GA, Chen C, Kalady M & Reed JF 3rd (1997). Thigh muscle size and strength after anterior cruciate ligament reconstruction and rehabilitation. *J Orthop Sports Phys Ther* **26**, 238–243.
- Baar K & Esser K (1999). Phosphorylation of p70^{S6k} correlates with increased skeletal muscle mass following resistance exercise. *Am J Physiol Cell Physiol* **276**, C120–C127.
- Balogh K (1970). Corrective massage for atrophic masticatory and mimetic muscles. *Dent Dig* **76**, 347–348.
- Brack AS & Rando TA (2012). Tissue-specific stem cells: lessons from the skeletal muscle satellite cell. *Cell Stem Cell* **10**, 504–514.
- Busch R, Kim YK, Neese RA, Schade-Serin V, Collins M, Awada M, Gardner JL, Beysen C, Marino ME, Misell LM & Hellerstein MK (2006). Measurement of protein turnover rates by heavy water labeling of nonessential amino acids. *Biochim Biophys Acta* **1760**, 730–744.
- Butterfield TA, Zhao Y, Agarwal S, Haq F & Best TM (2008). Cyclic compressive loading facilitates recovery after eccentric exercise. *Med Sci Sports Exerc* **40**, 1289–1296.
- Cafarelli E & Flint F (1992). The role of massage in preparation for and recovery from exercise. An overview. *Sports Med* **14**, 1–9.
- Carroll TJ, Herbert RD, Munn J, Lee M & Gandevia SC (2006). Contralateral effects of unilateral strength training: evidence and possible mechanisms. *J Appl Physiol (1985)* **101**, 1514–1522.
- Catoire M & Kersten S (2015). The search for exercise factors in humans. *FASEB J* **29**, 1615–1628.
- Crane JD, Ogborn DI, Cupido C, Melov S, Hubbard A, Bourgeois JM & Tarnopolsky MA (2012). Massage therapy attenuates inflammatory signaling after exercise-induced muscle damage. *Sci Transl Med* **4**, 119ra113.
- Crossland H, Kazi AA, Lang CH, Timmons JA, Pierre P, Wilkinson DJ, Smith K, Szewczyk NJ & Atherton PJ (2013). Focal adhesion kinase is required for IGF-I-mediated growth of skeletal muscle cells via a TSC2/mTOR/S6K1-associated pathway. *Am J Physiol Endocrinol Metab* **305**, E183–E193.
- Cui C & Tseng H (2004). Estimation of ribosomal RNA transcription rate in situ. *Biotechniques* **36**, 134–138.
- Drake JC, Peelor FF 3rd, Biela LM, Watkins MK, Miller RA, Hamilton KL & Miller BF (2013). Assessment of mitochondrial biogenesis and mTORC1 signaling during chronic rapamycin feeding in male and female mice. *J Gerontol A Biol Sci Med Sci* **68**, 1493–1501.
- Drake JC, Bruns DR, Peelor FF 3rd, Biela LM, Miller RA, Miller BF & Hamilton KL (2015). Long-lived Snell dwarf mice display increased proteostatic mechanisms that are not dependent on decreased mTORC1 activity. *Aging cell* **14**, 474–482.
- Drake JC, Bruns DR, Peelor FF 3rd, Biela LM, Miller RA, Hamilton KL & Miller BF (2014). Long-lived crowded-litter mice have an age-dependent increase in protein synthesis to DNA synthesis ratio and mTORC1 substrate phosphorylation. *Am J Physiol Endocrinol Metab* **307**, E813–821.
- Dupont-Versteegden EE, Murphy RJ, Houle JD, Gurley CM & Peterson CA (1999). Activated satellite cells fail to restore myonuclear number in spinal cord transected and exercised rats. *Am J Physiol* **277**, C589–C597.
- Eftestol E, Egner IM, Lunde IG, Ellefsen S, Andersen T, Sjaland C, Gundersen K & Bruusgaard JC (2016). Increased hypertrophic response with increased mechanical load in skeletal muscles receiving identical activity patterns. *Am J Physiol Cell Physiol* **311**, C616–C629.
- Files DC, Sanchez MA & Morris PE (2015). A conceptual framework: the early and late phases of skeletal muscle dysfunction in the acute respiratory distress syndrome. *Crit Care* **19**, 266.

- Fry CS, Lee JD, Jackson JR, Kirby TJ, Stasko SA, Liu H, Dupont-Versteegden EE, McCarthy JJ & Peterson CA (2014). Regulation of the muscle fiber microenvironment by activated satellite cells during hypertrophy. *FASEB J* **28**, 1654–1665.
- Galleghy JC, Turesky NA, Strotman BA, Gurley CM, Peterson CA & Dupont-Versteegden EE (2004). Satellite cell regulation of muscle mass is altered at old age. *J Appl Physiol* **97**, 1082–1090.
- Gan B, Yoo Y & Guan JL (2006). Association of focal adhesion kinase with tuberous sclerosis complex 2 in the regulation of s6 kinase activation and cell growth. *J Biol Chem* **281**, 37321–37329.
- Gibson MC & Schultz E (1983). Age-related differences in absolute numbers of skeletal muscle satellite cells. *Muscle Nerve* **6**, 574–580.
- Goodman CA, Kotecki JA, Jacobs BL & Hornberger TA (2012). Muscle fiber type-dependent differences in the regulation of protein synthesis. *PLoS One* **7**, e37890.
- Gordon SE, Fluck M & Booth FW (2001). Selected Contribution: Skeletal muscle focal adhesion kinase, paxillin, and serum response factor are loading dependent. *J Appl Physiol* (1985) **90**, 1174–1183; discussion 1165.
- Graham ZA, Gallagher PM & Cardozo CP (2015). Focal adhesion kinase and its role in skeletal muscle. *J Muscle Res Cell Motil* **36**, 305–315.
- Grebien F, Dolznig H, Beug H & Mullner EW (2005). Cell size control: new evidence for a general mechanism. *Cell Cycle* **4**, 418–421.
- Hynes RO (2002). Integrins: bidirectional, allosteric signaling machines. *Cell* **110**, 673–687.
- Ishido M, Uda M, Kasuga N & Masuhara M (2009). The expression patterns of Pax7 in satellite cells during overload-induced rat adult skeletal muscle hypertrophy. *Acta Physiol (Oxf)* **195**, 459–469.
- Jackson JR, Kirby TJ, Fry CS, Cooper RL, McCarthy JJ, Peterson CA & Dupont-Versteegden EE (2015). Reduced voluntary running performance is associated with impaired coordination as a result of muscle satellite cell depletion in adult mice. *Skelet Muscle* **5**, 41.
- Jackson JR, Mula J, Kirby TJ, Fry CS, Lee JD, Ubele MF, Campbell KS, McCarthy JJ, Peterson CA & Dupont-Versteegden EE (2012). Satellite cell depletion does not inhibit adult skeletal muscle regrowth following unloading-induced atrophy. *Am J Physiol Cell Physiol* **303**, C854–C861.
- Jay K, Sundstrup E, Sondergaard SD, Behm D, Brandt M, Saervoll CA, Jakobsen MD & Andersen LL (2014). Specific and cross over effects of massage for muscle soreness: randomized controlled trial. *Int J Sports Phys Ther* **9**, 82–91.
- Katsumi A, Orr AW, Tzima E & Schwartz MA (2004). Integrins in mechanotransduction. *J Biol Chem* **279**, 12001–12004.
- Khan MM, Lustrino D, Silveira WA, Wild F, Straka T, Issop Y, O'Connor E, Cox D, Reischl M, Marquardt T, Labeit D, Labeit S, Benoit E, Molgo J, Lochmuller H, Witzemann V, Kettelhut IC, Navegantes LC, Pozzan T & Rudolf R (2016). Sympathetic innervation controls homeostasis of neuromuscular junctions in health and disease. *Proc Natl Acad Sci USA* **113**, 746–750.
- Lee JJ, Waak K, Grosse-Sundrup M, Xue F, Lee J, Chipman D, Ryan C, Bittner EA, Schmidt U & Eikermann M (2012). Global muscle strength but not grip strength predicts mortality and length of stay in a general population in a surgical intensive care unit. *Phys Ther* **92**, 1546–1555.
- Marcotte GR, West DW & Baar K (2015). The molecular basis for load-induced skeletal muscle hypertrophy. *Calcif Tissue Int* **96**, 196–210.
- Mathew SJ, Hansen JM, Merrell AJ, Murphy MM, Lawson JA, Hutcheson DA, Hansen MS, Angus-Hill M & Kardon G (2011). Connective tissue fibroblasts and Tcf4 regulate myogenesis. *Development* **138**, 371–384.
- McCarthy JJ, Mula J, Miyazaki M, Erfani R, Garrison K, Farooqui AB, Srikuea R, Lawson BA, Grimes B, Keller C, Van Zant G, Campbell KS, Esser KA, Dupont-Versteegden EE & Peterson CA (2011). Effective fiber hypertrophy in satellite cell-depleted skeletal muscle. *Development* **138**, 3657–3666.
- McGlory C, Devries MC & Phillips SM (2017). Skeletal muscle and resistance exercise training; the role of protein synthesis in recovery and remodelling. *J Appl Physiol* (1985) **122**, 541–548.
- McKay WP, Jacobson P, Chilibeck PD & Daku BL (2006). Effects of graded levels of exercise on ipsilateral and contralateral post-exercise resting rectus femoris mechanomyography. *Eur J Appl Physiol* **98**, 566–574.
- Metter EJ, Talbot LA, Schrager M & Conwit R (2002). Skeletal muscle strength as a predictor of all-cause mortality in healthy men. *J Gerontol A Biol Sci Med Sci* **57**, B359–B365.
- Miller BF, Drake JC, Naylor B, Price JC & Hamilton KL (2014). The measurement of protein synthesis for assessing proteostasis in studies of slowed aging. *Ageing Res Rev* **18**, 106–111.
- Miller BF, Robinson MM, Reuland DJ, Drake JC, Peelor FF 3rd, Bruss MD, Hellerstein MK & Hamilton KL (2013). Calorie restriction does not increase short-term or long-term protein synthesis. *J Gerontol A Biol Sci Med Sci* **68**, 530–538.
- Miller BF, Wolff CA, Peelor FF 3rd, Shipman PD & Hamilton KL (2015). Modeling the contribution of individual proteins to mixed skeletal muscle protein synthetic rates over increasing periods of label incorporation. *J Appl Physiol* (1985) **118**, 655–661.
- Morita M, Gravel SP, Hulea L, Larsson O, Pollak M, St-Pierre J & Topisirovic I (2015). mTOR coordinates protein synthesis, mitochondrial activity and proliferation. *Cell Cycle* **14**, 473–480.
- Munn J, Herbert RD & Gandevia SC (2004). Contralateral effects of unilateral resistance training: a meta-analysis. *J Appl Physiol* (1985) **96**, 1861–1866.
- Navegantes LC, Resano NM, Baviera AM, Migliorini RH & Kettelhut IC (2004). Effect of sympathetic denervation on the rate of protein synthesis in rat skeletal muscle. *Am J Physiol Endocrinol Metab* **286**, E642–E647.
- Rantanen T, Harris T, Leveille SG, Visser M, Foley D, Masaki K & Guralnik JM (2000). Muscle strength and body mass index as long-term predictors of mortality in initially healthy men. *J Gerontol A Biol Sci Med Sci* **55**, M168–M173.
- Robertson RT, Levine ST, Haynes SM, Gutierrez P, Baratta JL, Tan Z & Longmuir KJ (2015). Use of labeled tomato lectin for imaging vasculature structures. *Histochem Cell Biol* **143**, 225–234.

- Schmalbruch H & Hellhammer U (1977). The number of nuclei in adult rat muscles with special reference to satellite cells. *Anat Rec* **189**, 169–175.
- Shenker N, Haigh R, Roberts E, Mapp P, Harris N & Blake D (2003). A review of contralateral responses to a unilateral inflammatory lesion. *Rheumatology (Oxford)* **42**, 1279–1286.
- Song Y, Forsgren S, Yu J, Lorentzon R & Stal PS (2012). Effects on contralateral muscles after unilateral electrical muscle stimulation and exercise. *PLoS One* **7**, e52230.
- Spangenburg EE (2009). Changes in muscle mass with mechanical load: possible cellular mechanisms. *Appl Physiol Nutr Metab* **34**, 328–335.
- Srikanthan P & Karlamangla AS (2014). Muscle mass index as a predictor of longevity in older adults. *Am J Med* **127**, 547–553.
- Suskind MI, Hajek NM & Hines HM (1946). Effects of massage on denervated skeletal muscle. *Arch Phys Med Rehabil* **27**, 133–135.
- Tidball JG (2005). Mechanical signal transduction in skeletal muscle growth and adaptation. *J Appl Physiol (1985)* **98**, 1900–1908.
- Tomakidi P, Schulz S, Proksch S, Weber W & Steinberg T (2014). Focal adhesion kinase (FAK) perspectives in mechanobiology: implications for cell behaviour. *Cell Tissue Res* **357**, 515–526.
- Waters-Banker C, Butterfield TA & Dupont-Versteegden EE (2014a). Immunomodulatory effects of massage on nonperturbed skeletal muscle in rats. *J Appl Physiol* **116**, 164–175.
- Waters-Banker C, Dupont-Versteegden EE, Kitzman PH & Butterfield TA (2014b). Investigating the mechanisms of massage efficacy: the role of mechanical immunomodulation. *J Athl Train* **49**, 266–273.
- Westerkamp CM & Gordon SE (2005). Angiotensin-converting enzyme inhibition attenuates myonuclear addition in overloaded slow-twitch skeletal muscle. *Am J Physiol Regul Integr Comp Physiol* **289**, R1223–R1231.
- White JR, Confides AL, Moore-Reed S, Hoch JM & Dupont-Versteegden EE (2015). Regrowth after skeletal muscle atrophy is impaired in aged rats, despite similar responses in signaling pathways. *Exp Gerontol* **64**, 17–32.
- Wolfe RR (2006). The underappreciated role of muscle in health and disease. *Am J Clin Nutr* **84**, 475–482.
- Yue G & Cole KJ (1992). Strength increases from the motor program: comparison of training with maximal voluntary and imagined muscle contractions. *J Neurophysiol* **67**, 1114–1123.
- Zhou S (2000). Chronic neural adaptations to unilateral exercise: mechanisms of cross education. *Exerc Sport Sci Rev* **28**, 177–184.
- Zou K, Huntsman HD, Carmen Valero M, Adams J, Skelton J, De Lisio M, Jensen T & Boppard MD (2015). Mesenchymal stem cells augment the adaptive response to eccentric exercise. *Med Sci Sports Exerc* **47**, 315–325.

Additional information

Author's present address

Z. R. Majeed: Department of Biology, College of Science, Salahaddin University-Erbil, Erbil, Iraq.

Competing interests

The authors declare that they do not have any competing interests associated with this work.

Author contributions

All experimentation was performed at the University of Kentucky, except for the analysis of protein and DNA synthesis and western analysis for ERK1/2 and rps6, which was performed at Colorado State University. B.M. and K.H. were responsible for acquisition, analysis and interpretation of data and for critically revising the manuscript; Z.M. contributed to the acquisition, analysis and interpretation of the work; S.A., A.C., A.H., E.H., P.S. and F.P. were responsible for acquisition, analysis and interpretation of data; T.B. and E.D.V. were responsible for conception and design of the experiments, for interpretation of the results and drafting and revising the manuscript. All authors have approved the final version of the manuscript and agree to be accountable for all aspects of the work. All persons designated as authors qualify for authorship, and all those who qualify for authorship are listed.

Acknowledgements

This work was supported by NIH grants AT009268 and AG042699 (E.D., T.B.), and AG-042569 (B.M., K.H.). A.H. was supported by an undergraduate research summer fellowship from the American Physiological Society. We would like to thank Kathryn Baeverstadt for technical support.

Translational perspective

Muscle mass and strength are highly correlated with morbidity and mortality and are predictive of functional outcomes during hospital stay, particularly after ICU admission (Lee *et al.* 2012). Muscle weakness and lack of recovery of muscle size after a period of disuse, such as bed rest, carries a large monetary burden and contributes to a decrease in quality of life for those affected. In addition, muscle loss after orthopaedic surgeries, such as ACL repair, does quite often not fully recover, leading to impairment of those affected with this atrophy (Arangio *et al.* 1997). An intervention such as massage, that can shift the protein homeostatic balance to synthesis over degradation, is easily applicable clinically, and can be initiated early when the protein loss is largest, has the potential to make a large impact on the clinical outcomes of those affected by muscle atrophy (Files *et al.* 2015). In addition, we propose that massage in combination with other anabolic stimuli, such as ingestion of essential amino acids, may have an even larger effect.